Structural Analysis of Sulfated Glycans by Sequential Double-Permethylation Using Methyl Iodide and Deuteromethyl Iodide

Ming Lei, Yehia Mechref, and Milos V. Novotny
National Center of Glycomics and Glycoproteomics and Department of Chemistry, Indiana University, Bloomington, Indiana, USA

MALDI mass spectrometric characterization of sulfated glycans is often challenging due to their low ionization response in the positive ion mode. Here we demonstrate a new analytical approach, allowing the measurement of sulfated glycans by substituting the sulfate group with a deuteromethyl group. Sulfated glycan samples are initially permethylated before the methanolytic cleavage of their sulfate groups. Desulfated and permethylated glycans are then subjected to another permethylation step using deuteromethyl iodide to label the hydroxyl groups resulting from methanolysis. The number of attached sulfate groups is subsequently calculated from the mass-shift resulting from the chemical cleavage of these sulfate groups. The position of the sulfate substitution is then determined by collision-induced dissociation (CID) tandem mass spectrometry of permethylated and permethylated plus deuteromethylated samples. The described approach was initially optimized and validated using linear standard glycans, while its effectiveness has also been demonstrated here for the N-glycans derived from bovine thyroid-stimulating hormone (bTSH).   (J Am Soc Mass Spectrom 2009, 20, 1660–1671) © 2009 American Society for Mass Spectrometry

Glycosylation is one of the most prevailing and versatile protein post-translational modifications. The structure and abundance of each glycan can play an important role in many biological functions, such as the cellular recognition processes. Consequently, altered glycan structures and their relative abundance could be attributes of many diseases, including cancer, immune system dysfunction and growth inhibition [1–3]. Moreover, some glycan structures possess polar moieties, such as sialylation and sulfation. The latter has already been implicated in diseases, such as neural system dysfunctions [4] and cancer [1, 5, 6]. An improved understanding of the biologic roles of sulfated glycans and their disease connections necessitates definitive structural determination and precise analytical measurements which can potentially lead to the discovery of new disease biomarkers [1, 3].

Nuclear magnetic resonance (NMR) spectrometry [7, 8] and ^{34}S isotopic labeling [9–11] have been previously considered to be the main methodologies in the structural analysis of sulfated glycoconjugates. However, the low sensitivity of NMR and the need to use hazardous chemicals in the case of the latter, make these approaches less desirable than mass spectrometry (MS). In principle, MS measurements provide high sensitivity, wide applicability, and the capability of high-throughput investigations. However, structural analysis and quantitative measurements of sulfated glycans are analytically challenging. The matrix-assisted laser desorption/ionization (MALDI)-MS signals of sulfated glycans are usually suppressed in the positive-ion mode because of their low ionization efficiency relative to their neutral counterparts [12]. Sulfate groups are commonly cleaved during MALDI-MS ionization process, thus making the determination of a sulfate group position difficult [13–15]. In the case of electrospray ionization (ESI)-MS, the loss of sulfate group is not observed but the signal intensity of glycans are generally lower than that of MALDI [16, 17]. These obstacles could be partially overcome through the use of negative-ion MS, as the negative charge can be retained on sulfated glycans, thus making them amenable to ionization as well as tandem MS analysis [17–19]. However, additional problems limit the potential use of this approach, including lower sensitivity and signal suppression of the less acidic species, such as sialylated glycans [20, 21]. Additionally, it is inherently difficult to simultaneously analyze neutral and sulfated glycans in the negative-ion mode. Nevertheless, several attempts have been made to characterize sulfated glycans by MS [22–24]. For example, a tripeptide Lys-Lys-Lys was employed as an ion-pairing reagent to complex with the sulfated compounds, thus enhancing their ionization efficiency [22–24].

Here, we introduce a different approach involving double-permethylation to improve the characterization

Address reprint requests to Dr. Y. Mechref and Dr. M. V. Novotny, Department of Chemistry, Indiana University, 800 E. Kirkwood Ave., Bloomington, IN 47405, USA. E-mail: ymechref@indiana.edu and E-mail: novotny@indiana.edu

of sulfated glycans by positive-ion mode MALDI-MS and potentially address the aforementioned analytical challenges. Samples are first permethylated, leaving the sulfate group intact [25, 26]. This permethylation step also stabilizes sialylated structures during methanolysis [27] and the MS process [28]. The sulfate group is then cleaved by mild acidic methanolysis, while the hydroxyl groups formed as a result of this cleavage are either permethylated or deuteromethylated. As a result of this treatment, the sulfate group is substituted by a deuterom-ethyl group which is stable during MALDI-MS analysis. This permethylation step also improves and enhances MS ionization and fragmentation [29, 30]. The num-ber of sulfate groups associated with a particular glycan can be deduced from the mass-shift observed through comparing the spectra of permethylated and doubly-permethylated compounds. The position of a sulfate group can also be determined by comparing the collision-induced dissociation (CID) spectra of the two doubly-permethylated samples, using methyl iodide and deuteromethyl iodide. This method was optimized and validated using sulfated oligosaccharide standards, while its application was demonstrated for glycans released from bovine thyroid-stimulating hormone (bTSH), a well-characterized glycoprotein [31–34].

Experimental

Materials

Di- and trisulfated oligosaccharide standards were purchased from V-labs (Covington, LA, USA). Bovine thyroid-stimulating hormone (bTSH), peptide: N-glycosidase F (PNGase F), sodium dodecyl sulfate (SDS), octyl phenoxylpolyethoxylethanol, a nonionic nondenaturing detergent (NP-40), and the MALDI ma-trix, 2,5-dihydroxybenzoic acid (DHB) were purchased from Sigma-Aldrich (Milwaukee, WI, USA). Chloro-form, methyl iodide, dimethylsulfoxide (DMSO) and sodium chloride were received from EM Science (Gibbstown, NJ, USA).

Methanolic Desulfation

Methanolic desulfation was a modified version of the method originally described by Taguchi et al. [25] Briefly, 0.05 M anhydrous methanol/HCl was prepared by reacting $MgSO_4$-dried methanol with acetylchloride. Next, vacuum-dried glycan sample was resuspended in 10 μL 0.05 M methanol/HCl solution and allowed to react at room temperature for 2 h. The reaction was stopped by neutralizing the solution on ice with 0.05 M methanol/NaOH solution. One nmol of each oligosac-charide standard were used for method optimization and 100 μg (2 nmol) bTSH glycoprotein was used for method validation.

Release of N-Glycans from Bovine Thyroid-stimulating Hormone (bTSH)

The N-glycans were released from the bTSH glycopro-tein employing PNGase F, according to our previously published procedure [35]. Briefly, an aliquot of bTSH glycoprotein (100 μg, 2 nmol) was dissolved in 50 μL 100 mM phosphate buffer (pH 7.5) containing 0.5% SDS and heated in water bath at 95 °C for 10 min. Then, NP-40 was added to neutralize the negative charges of SDS before the addition of PNGase F. Sample was then incubated at 37 °C overnight. Next, PNGase F was added again and the reaction was allowed to proceed for additional 4 h at 37 °C. Finally, samples were vacuum-dried before permethylation.

Permethylation and Deuteromethylation

Solid-phase permethylation and deuteropermethyla-tion was performed according to our previously pub-lished procedure [29, 30, 36]. Briefly, NaOH beads were packed in a spin column to about 3 cm depth using acetonitrile. The spin column was then centrifuged and washed several times with 50-μL aliquots of DMSO. Vacuum-dried sulfated oligosaccharide standard (1 nmol) and N-glycans derived from bTSH (100 μg of glycoprotein, 2 nmol) were then dissolved in 90 μL DMSO and 40 μL methyl iodide (or deuteromethyl iodide). A 1-μL aliquot of water was also added to prevent peeling reactions [37]. The sample solution was then centrifuged at low speed. Samples were recycled through the spin column eight times. The spin column was finally washed with an additional 50-μL aliquot of DMSO.

C_{18} Extraction

A 2-mL aliquot of 0.1% trifluoroacetic acid (TFA) aque-ous solution was added to permethylated samples before solid-phase extraction using preconditioned C_{18} cartridges. TFA was used here as an ion-pairing agent. Solid-phase C_{18} cartridges were pre-conditioned with a 2-mL ethanol aliquot and a 2-mL water aliquot. After applying samples, cartridges were washed with a 2-mL water aliquot, while permethylated sugars were eluted with a 1.8-mL aliquot of 90:5:5 ACN:water:isopropanol solution. Eluent was dried under vacuum.

MALDI Mass Spectrometry

Mass-spectrometric analyses were performed using an Applied Biosystems 4800 Proteomics Analyzer (Applied Biosystems, Framingham, MA). The Nd:YAG laser of this instrument provides a power input at 355 nm. MS data were further processed using DataExplorer 4.6 (Applied Biosystems).

Positive MALDI-CID spectra were acquired using the same instrument. Collision energy was set to 1 kV, as defined by the potential difference between the
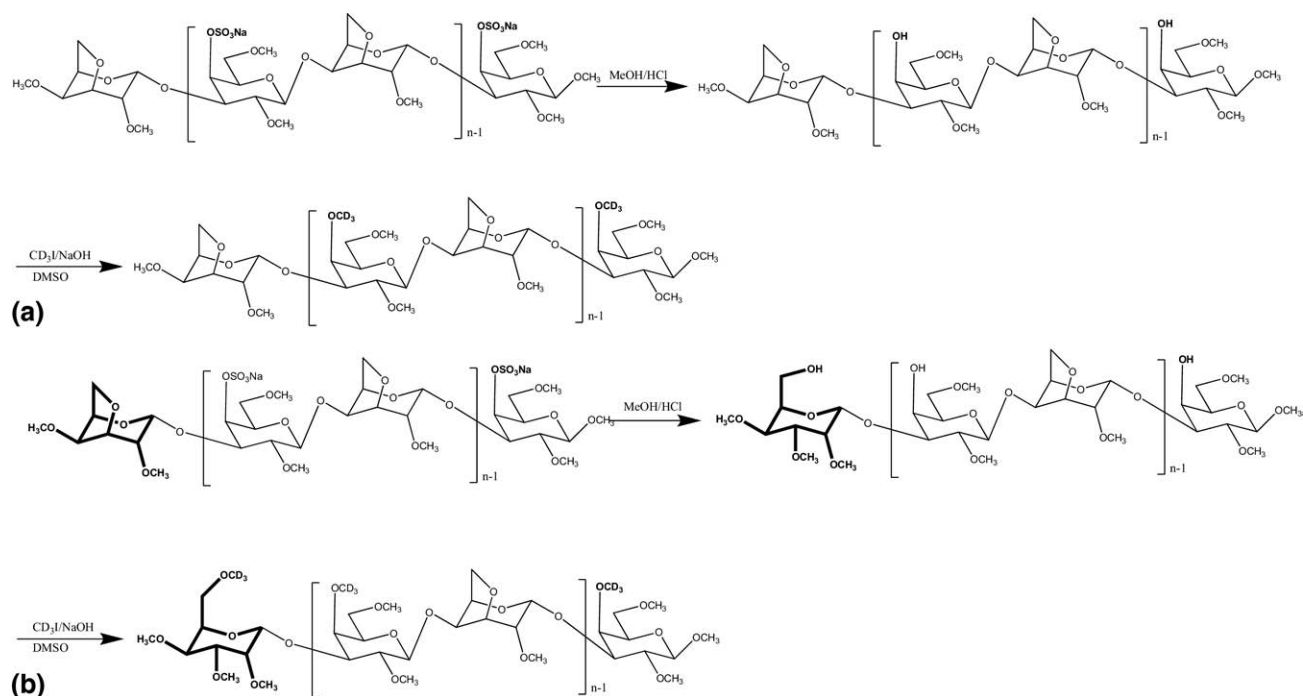
Figure 1. Illustration of double-permethylation on (**a**) permethylated sulfated oligosaccharide standard and (**b**) the side reaction involves the methanolysis of 3,6-anhydrogalactose residue specific for this structure. The reaction shown here is on the non-reducing end for representation; however, the actual site of reaction was not determined; n is the number of sulfate groups attached.

source and the collision cell. Air was used as the collision gas at a pressure of 8.0×10^{-6} torr to enhance cross-ring fragmentation of sugar molecules.

Vacuum-dried samples were re-suspended in 1:1 methanol:water solution and mixed with 2,5-DHB matrix at 1:1 ratio. Matrix was prepared at 10 mg/mL concentration through dissolving appropriate amount of 2,5-DHB in a 1:1 methanol:water solution containing 2 mM sodium acetate. This small amount of sodium acetate is needed to ensure the formation of sodium adducts.

Results and Discussion

Optimization of Double-permethylation Using Sulfated Oligosaccharide Standard

The critical step of the approach described here is the methanolysis desulfation, which was originally described by Taguchi et al. [25]. This reaction results in the loss of sulfate groups as illustrated in Figure 1a. Although this protocol was previously described, we still had to optimize and validate its efficiency using a permethylated, disulfated, and trisulfated oligosaccharide standard. The reported protocol calls for incubation of sulfated glycans in 0.5 M methanol/HCl solution for 2 h at room temperature. However, under these conditions, no detectable peak associated with the desulfated structures was observed (data not shown). Nevertheless, several peaks were observed in the low m/z unit range, which are believed to originate from the cleavage of the glycosidic bonds. Such cleavages are prompted by the highly acidic condition of this reaction.

Therefore, optimization of the desulfation reaction was attained through a time titration using MeOH/HCl solution at a 10-fold lower concentration on a permethylated trisulfated oligosaccharide standard (m/z unit
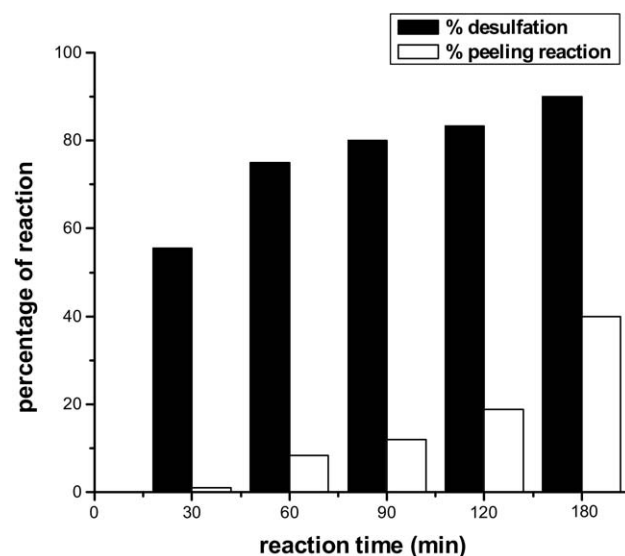

Figure 2. Percentage of desulfation (methanolysis) and peeling reactions with respect to their reaction times. The completeness of desulfation was calculated as the intensity of the total desulfated peak (if more than one sulfate group is present) divided by the intensity sum of all peaks corresponding to desulfation reaction, including unreacted, partially-reacted, and final product. The percentage of peeling reaction was then calculated with respect to the percentage of final product.

1419.4). The bar graphs shown in Figure 2 demonstrate the efficiency of desulfation as well as the extent of peeling reactions resulting from glycosidic bond cleavages. A 1.2-nmol aliquot of the sample was allowed to react, while MALDI mass spectrum of an aliquot of the reaction mixture was acquired every 30 min for 2.5 h. The observed peaks associated with the reaction included a completely desulfated peak (m/z unit 1113.5), a partially desulfated peak resulting from the loss of two sulfate group (m/z unit 1215.4), a peak resulting from glycosidic bond cleavage (m/z unit 1104.9), and certain peaks originating from side reaction due to the methanolysis of the dehydrated non-reducing end of the standard oligosaccharides (m/z unit 1145.5 and 1247.4). The side reaction peaks were observed at m/z unit values higher than the expected products by 32 units,

resulting from the inclusion of $-OCH_3$ and $-H$ as illustrated in Figure 1b. This side reaction will not occur in the case of natural animal glycans, which do not possess epoxy functional group. Therefore, to better assess the efficiency of desulfation reaction in the absence of the dehydrated structures, the reaction efficiency was calculated by dividing the total intensity of the completely desulfated peak (m/z unit 1113.5) and its methanolyzed peak (m/z unit 1145.5) by the total intensity of the above mentioned peaks observed in the spectrum. Similarly, the extent of peeling reaction was monitored by dividing the intensity of the peak resulting from glycosidic bond cleavage (m/z unit 1104.9) by all the above mentioned peaks observed in the spectrum. Under the reaction conditions tested here, the cleavage of the sulfate groups and the glycosidic bonds
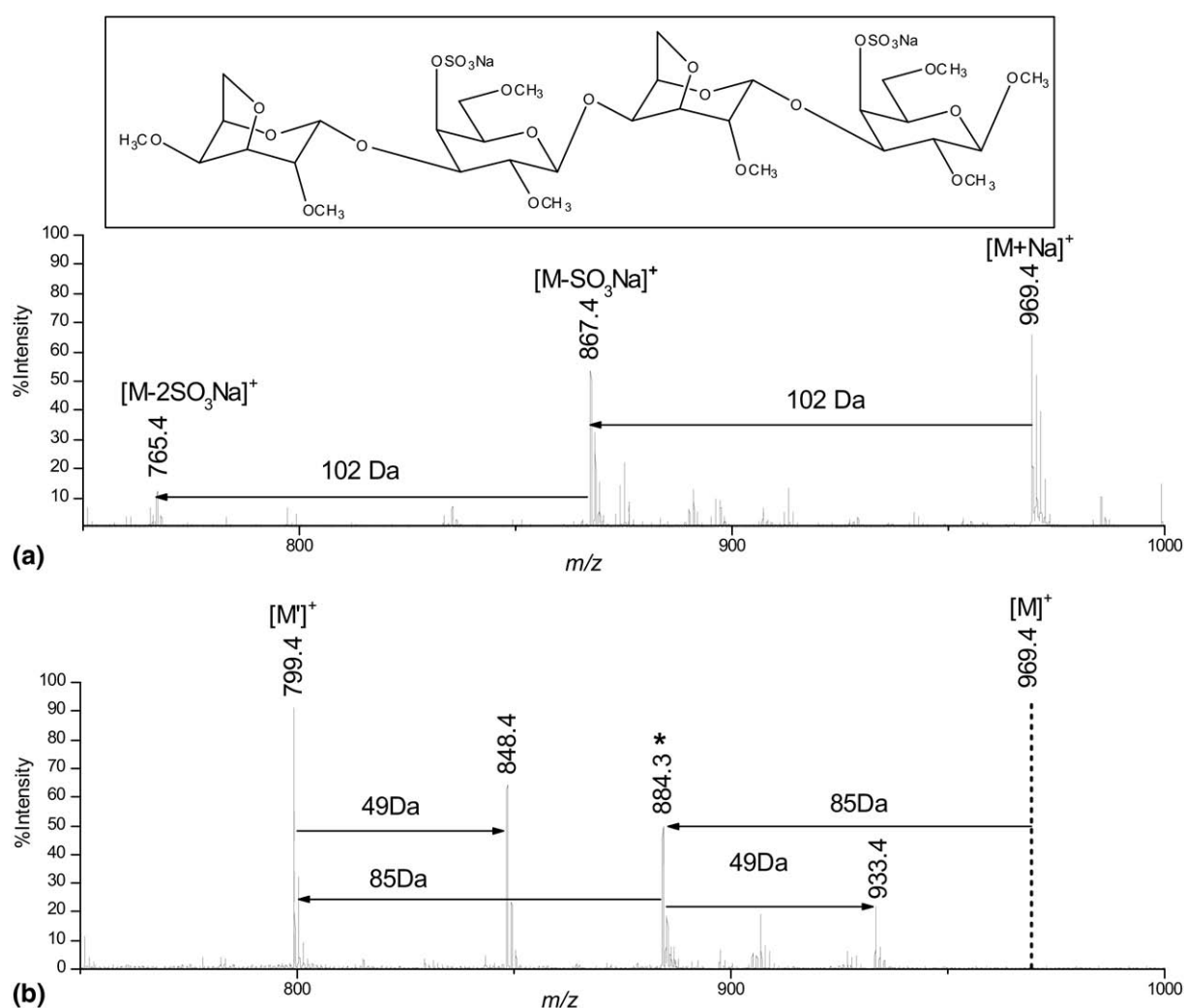

Figure 3. MALDI-MS spectra of disulfated oligosaccharide standards before (**a**) and after (**b**) double-permethylation derivatization. The structure of the oligosaccharide standard used is shown in the inserts of (**a**). Structures corresponding to peaks in (**b**) are listed in (**c**). The 102 Da shift represents a loss of sulfate group, while the 49 Da shift corresponding to the deuteromethylated molecule with the nonreducing end methanolyzed (Figure 1b). The 85 Da shift results from the substitution of $NaSO_3$ by CD_3 due to the treatment. M is the mass of native standard, while M' is the mass after double-permethylation. The peak marked with an asterisk represents the deuteropermethylated product from the incomplete cleavage of sulfate groups.

occurred simultaneously, but with different reaction efficiencies. Sulfate group cleavages proceeded at a faster rate relative to the glycosidic bond cleavages. Under the optimum conditions, effective desulfation must be attained with minimal glycosidic bond cleavages. Desulfation reaction reached 80% completion after 2.5 h, while the peeling reaction became significant after 2.5 h (Figure 2). Therefore, incubation of the analytes in 0.05 M methanol/HCl solution for 2 h at room temper-

ature yielded maximum desulfated products with minimum glycosidic bond cleavages.

MALDI mass spectra of the disulfated oligosaccharide standards subjected to double-permethylation are depicted in Figure 3. As a result of the desulfation of permethylated glycans and the deuteromethylation of the desulfated moieties, the peaks due to sulfated glycans were shifted to lower m/z unit values by $n \times 85$ units, where n represents the number of sulfate groups.
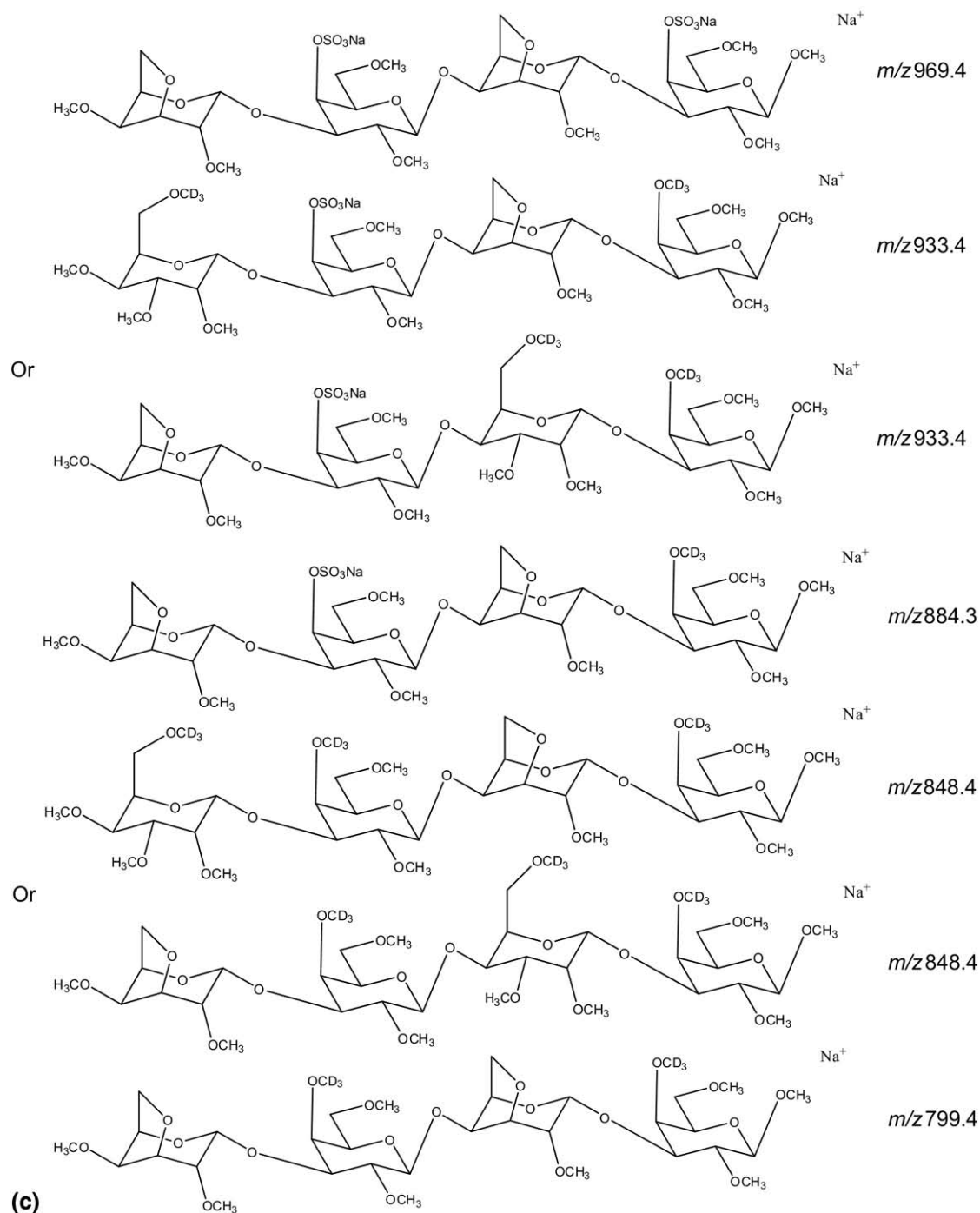
Figure 3. Continued.

This 85 m/z unit shift originates from the conversion of sodiated sulfate ($NaSO_3$) to a deuteromethyl group (CD_3) as a result of methanolysis desulfation and deuteropermethylation of the desulfated moieties. Therefore, the number of sulfate group associated with each glycan structure can be determined by calculating the m/z unit shift of the peaks observed in the permethylated and doubly-permethylated spectra. The MALDI mass spectrum of permethylated disulfated oligosaccharide standard is depicted in Figure 3a, while their structures are shown in Figure 3c. Although the MALDI ionization process is considered to be mild, post-source decay (PSD)

can also be observed for species containing labile bonds, such as acidic glycans [13–15]. Consequently, the losses of one and two sulfate groups are observed (m/z unit 867.4 and 765.5, respectively). The signal due to the ion originating from the loss of one sulfate group (m/z unit 867.4) is almost as intense as that of the parent ion (m/z unit 969.4), while the peaks originating from the loss of two sulfate groups are very weak (m/z unit 765.4).

Although no precursor ion of the disulfated permethylated oligosaccharide standard was observed after double-permethylation (Figure 3b), desulfation was not complete, as suggested by the detection of a peak at m/z
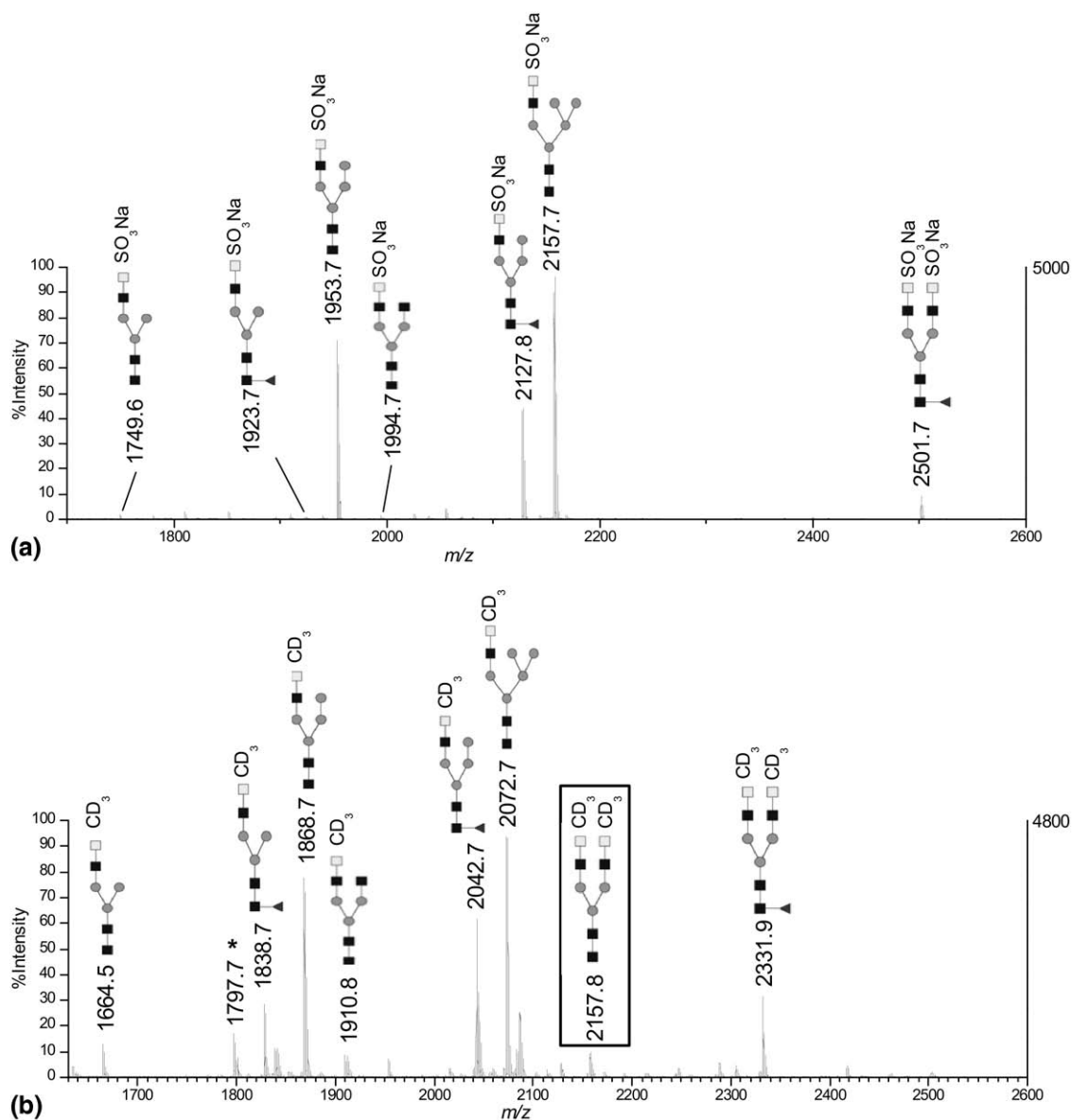

Figure 4. MALDI-MS of permethylated (**a**) and doubly-permethylated (**b**) bTSH N-glycans. Each spot contains ~50 pmol permethylated glycans. Structures of the identified sulfated glycans are labeled in the spectrum, while other peaks correspond to a partial permethylation and peeling reaction during methanolysis. A disulfated structure observed only after double-permethylation is framed. A peak due to the cleavage of terminal GalNAc is marked with an asterisk. A summary of all mass shifts can be found in Table 1. Key to symbols: [open square] GalNAc, [filled square] GlcNAc, [filled circle] mannose, [filled triangle] fucose.

unit 884.3 (M-1 × 85), corresponding to the loss of one sulfate group and deuteromethylation. Nevertheless, the most intense peak observed in the MALDI spectrum of doubly-permethylated sample at m/z unit 799.4 corresponds to the loss of two sulfate groups and the deuteromethylation of the desulfated sites (M-2 × 85). The signals observed at m/z unit values of 848.4 and 933.4 (Figure 3b), are associated with dehydrated 3,6-anhydrogalactose residue of the standard oligosaccharides described above (Figure 1b). MALDI-MS spectra were acquired between m/z unit values of 750 and 100 to exclude the matrix cluster peaks. The spectra depicted in Figure 3 were acquired using 100 pmol of disulfated oligosaccharide standard. Moreover, the peak intensities observed after double-permethylation were comparable to those observed after permethylation (data not shown), thus indicating a minimum sample loss.

Structural Analysis of Glycans Released from bTSH by Double-permethylation
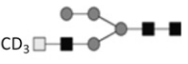
Thus far, we have demonstrated the potential of this double-permethylation protocol in the analysis of standard, linear sulfated glycans. The application of this protocol to the analysis of N-glycans derived from glyco-

proteins is illustrated for bTSH. This glycoprotein is well-characterized, containing mostly mono- and disulfated glycan structures [32–34]. Therefore, it is a good model glycoprotein to validate the double-permethylation protocol described above.

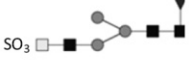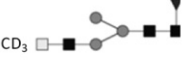bTSH N-glycans were released and doubly-permethylated as described above. After methanolysis, two equal aliquots were subjected to permethylation and deuteromethylation. These two aliquots were eventually subjected to both MALDI-MS and MALDI-CID-MS analyses. In the subsequent discussions, permethylated glycan will be referred to as P, permethylated-desulfated-permethylated as PP, and permethylated-desulfated-deuteromethylated as PD. MALDI mass spectra were acquired using the N-glycans derived from 5 μg (~100 pmol) bTSH.

As expected, the intensities of sulfated glycans moderately increased upon double-permethylation (Figure 4), thus suggesting the effectiveness of our approach and minimum sample loss. The observed signal also suggests a minimum sample loss associated with the chemical treatment. More importantly, a previously absent disulfated glycan (framed structure, Figure 4b) was observed before desulfation and deuteromethylation (compare Figure 4a and b). The possibility that

Table 1. Structure, observed m/z, and mass shifts for the glycans identified in permethylated (P) and doubly-permethylated (PD) samples. Bold and italicized contents highlight the observed structure only after double-permethylation (second row)

Permethylated (P)			Doubly-permethylated (PD)			
Compound structure	Calcd m/z [a]	Observed m/z	Compound structure	Calcd m/z	Observed m/z	Mass Shift [b]
	2501.9	2501.7		2332.0	2331.9	170 Da (2×85)
	2327.9	*N/A*		*2157.9*	*2157.8*	*170 Da (2×85)*
	2157.9	2157.7		2072.8	2072.7	85 Da (1×85)
	2127.9	2127.8		2042.8	2042.7	85 Da (1×85)
	1994.9	1994.7		1910.8	1910.6	85 Da (1×85)
	1953.9	1953.7		1868.8	1868.7	85 Da (1×85)
	1923.9	1923.7		1838.9	1838.7	85 Da (1×85)
	1749.8	1749.6		1664.7	1664.5	85 Da (1×85)

[a] All ions including the sulfate groups are sodiated unless otherwise annotated.
[b] 85Da is the mass difference between SO_3Na and CD_3.
Symbols: □ GalNAc, ■ GlcNAc, ● Mannose, △ Fucose

it is the defucosylated product of another specie (*m/z* unit 2331.9) can be excluded as the corresponding defucosylated peaks for other fucosylated structures (*m/z* unit 2127.8, 1934.7) was not found. Additionally, the defucosylated product of peak 2331.9 will be 3 Da higher than the observed peak as a result of the deuteropermethylation. Therefore, the detection of this structure suggests an enhancement in the ionization efficiency as a result of substituting the labile SO_3 group with the more stable CD_3 group. Moreover, it also proves that the recovery of this treatment is analytically satisfactory.

The cleavage of sulfate group appears to be analytically acceptable, since all the sulfated structures endured an $n \times 85$ *m/z* unit decrease, where *n* is representing the number of sulfate groups. Peaks originating

from the glycosidic bond cleavages were also observed; however, these peaks were exclusively corresponding to a cleavage of the sulfate-carrying monosaccharide. Example of these peaks is the one observed at *m/z* unit 1797.7 (PD), corresponding to biantennary monosulfated compound (*m/z* unit 2042.7 (PD)) with a cleaved terminal GalNAc (peak marked with asterisk, Figure 4b). However, the intensities of these signals were relatively weak. In addition, fucose moieties attached to the structure were intact, avoiding any possible confusion between fucosylated and sulfated structure since fucose attachment appears to be stable under the reaction condition [38]. Similarly, the sialic acid is also stable under the room temperature and mild acid conditions used here [27]. Therefore, the reaction condition described here has high specificity for sulfated structures.
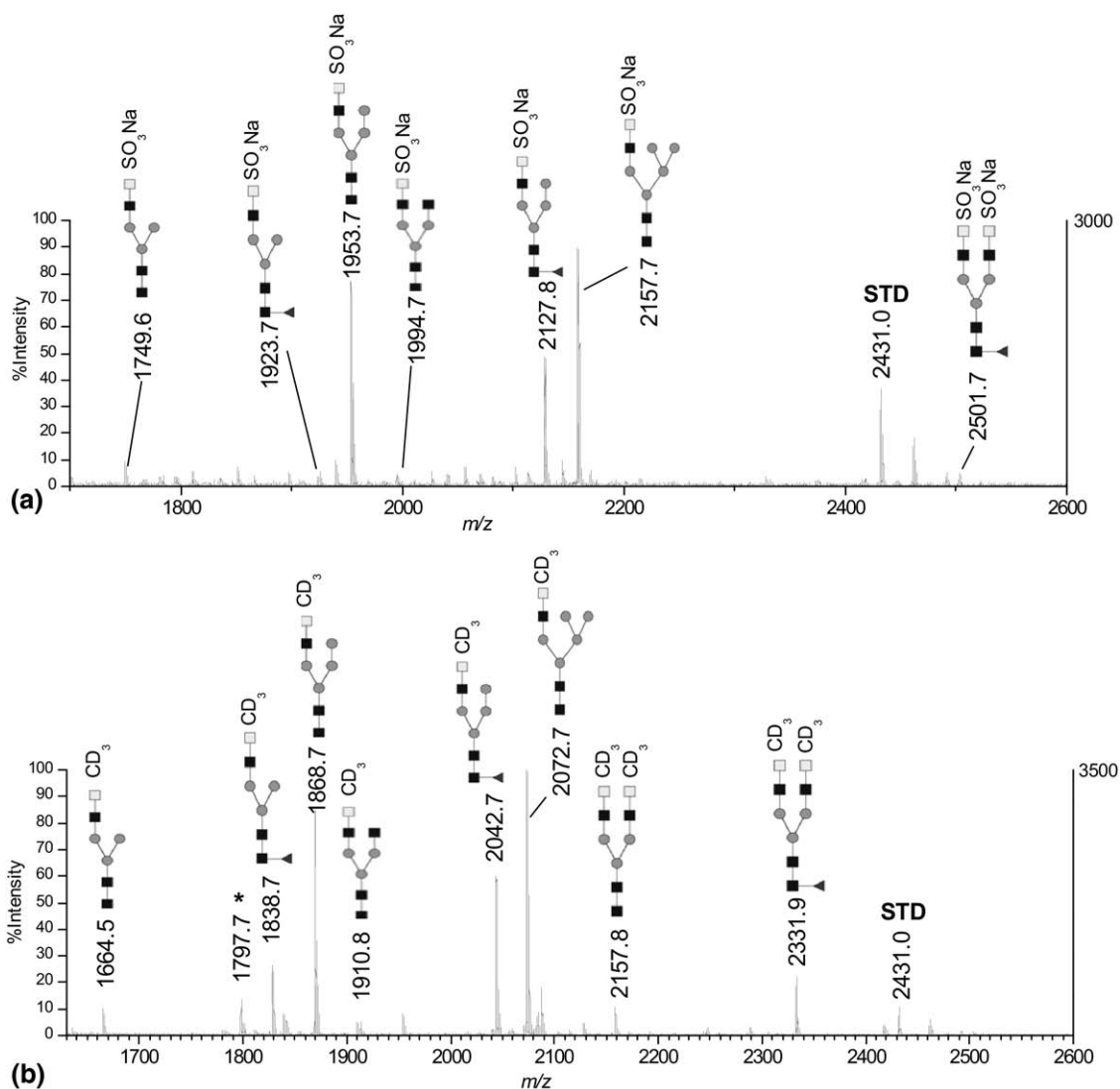
Figure 5. MALDI-MS spectra illustrating double permethylation efficiency. MALDI mass spectra of permethylated (**a**) and doubly-permethylated (**b**) bTSH N-glycans analyzed using an internal standard (*m/z* unit 2431.0). MALDI mass spectrum of permethylated and doubly permethylated bTSH N-glycans spotted in equal amounts (**c**). A peak due to the cleavage of terminal GalNAc is marked with an asterisk (**b**) and internal standard is labeled as STD. Table 2 summarizes the intensities of each bTSH N-glycan relative to that of the internal standard (*m/z* unit 2431.0).

The number of sulfate groups associated with each glycan was determined using the aforementioned calculation. The results were also confirmed by observing an $n \times 3$ m/z unit shift, when comparing PP and PD spectra (data not shown). The major glycans observed in the spectra depicted in Figure 4 were consistent with the structures previously reported [31–33]. The monosaccharide structures are adapted from Baenziger et al. [32]. The different sulfated structures and their corresponding m/z unit values are summarized in Table 1.

Evaluation of Signal Enhancement After Double-permethylation

To quantitatively evaluate the efficiency of our methodology, a sialylated complex-type N-glycan was used as an internal standard. The internal standard is permethylated and spotted with equal amount of P and PD bTSH N-glycan as shown in Figure 5a and b, respectively. The internal standard was observed as an intense peak at m/z unit 2431.0, the intensity of which was used for determining the efficiency of our approach. As depicted in Figure 5a and b, doubly-permethylated bTSH N-glycans showed higher intensities than that of permethylated glycans relative to the internal standard.

The intensity of each structure relative to that of the internal standard is listed in Table 2. The enhancement factor of double-permethylation is calculated by dividing the relative intensities of PD glycans with that of the P glycans. The intensities of monosulfated structures were approximately enhanced between 3.2 to 5 times as a result of the derivatization. The enhancement was more pronounced in the case of disulfated structures reaching a factor of 20. This is expected since polysulfated structures are more prone to in-source and post-source fragmentations as well as week ionization in MALDI positive-ion mode MS. The described derivatization approach allowed species with higher sulfation states to better ionize with minimum in-source and post-source fragmentations.

MALDI-CID Spectra of Biantennary Monosulfated Glycans

The position of sulfate groups can be determined by comparing MALDI-CID-MS spectra of PP and PD samples. The difference between the two precursor ions is $n \times 3$ m/z units. This difference is also observed for all product ions possessing the sulfation sites. Therefore, the site of sulfation can be potentially determined by comparing PP and PD CID-MS spectra. This is illus-

Table 2. Intensities of permethylated (P) and doubly-permethylated (PD) bTSH N-glycans relative to the intensity of the internal standard (m/z 2431.0)

Structure (P)	Relative intensity	Structure (PD)	Relative intensity	Enhancement factor
	0.3		1.0	3.3
	0.2		0.7	3.5
	1.8		5.7	3.2
	0.1		0.5	5.0
	1.2		4.0	3.3
	1.9		6.7	3.5
	0.05		1.0	20
	0.1		1.7	17
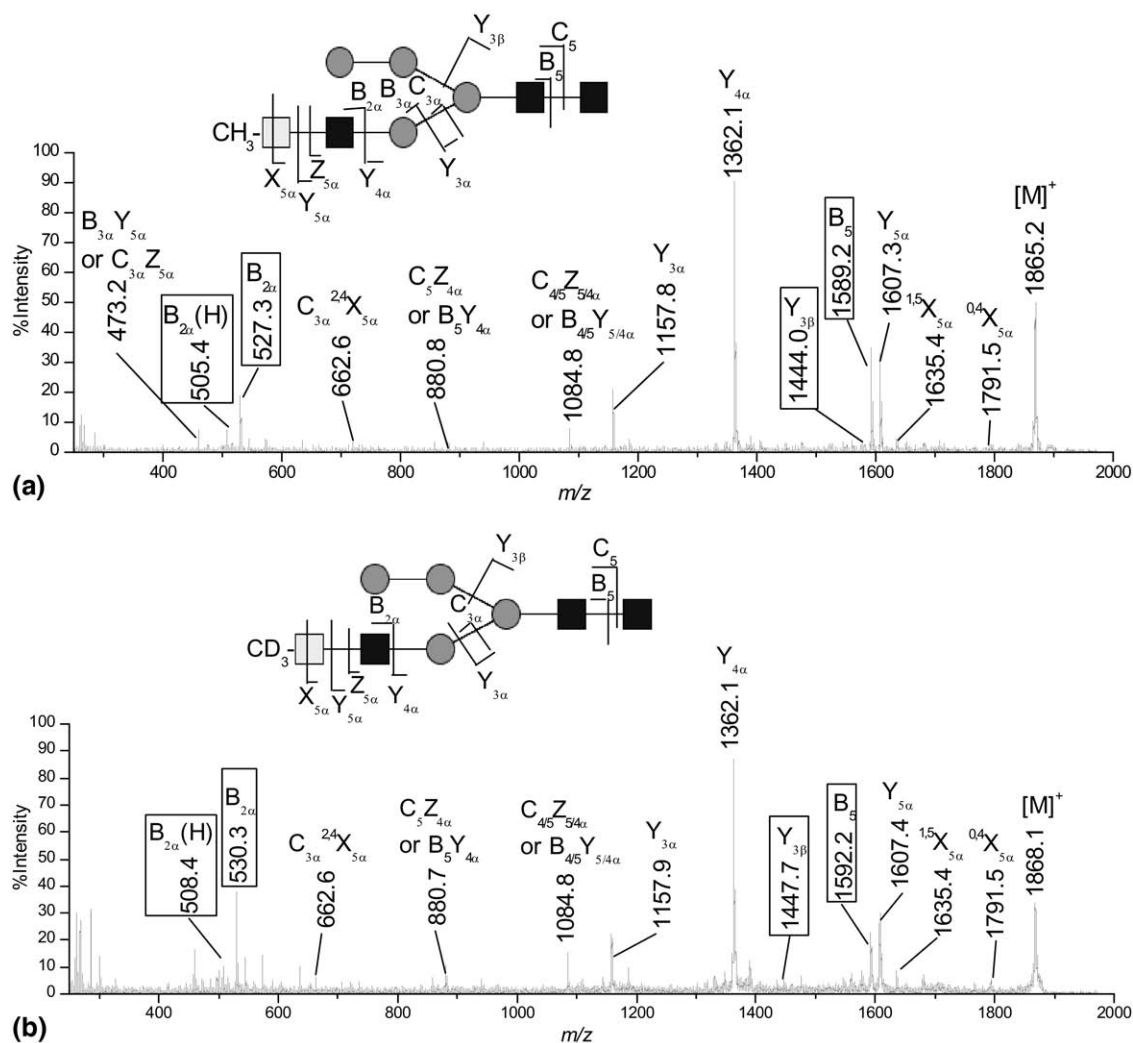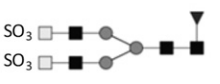
Figure 6. MS/MS (CID) spectra of (**a**) permethylated-permethylated (PP) and (**b**) permethylated-deuteromethylated (PD) mono-sulfated glycan from bTSH. All diagnostic ions for sulfate (with 3 Da difference) are framed. The position of CD_3 (sulfate) can be assigned to the 3 or 4 position of terminal HexNAc. All ions including the sulfate groups are sodiated unless otherwise annotated.

trated for a bi-antennary monosulfated glycan. The peak annotations of CID spectra follows the nomenclature proposed by Domon and Costello [39].

The m/z unit values of the two precursors depicted in Figure 6a (m/z unit 1865.2) and Figure 6b (m/z unit 1868.1) differ by 3 m/z units, suggesting the presence of a single sulfate group. Fragments representing a glycosidic bond dissociation (B, Y and C, Z ions) were the most abundant features, while some cross-ring fragmentations (A and X ions) were also observed, but only at lower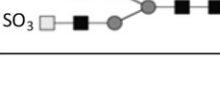 abundances (Figure 6). A complete B and Y ion series were observed on the α antenna (longest antenna), while only $Y_{3\beta}$ ion originating from the β antenna (theoretical m/z unit 1443.7) was observed at m/z unit values of 1444.0 in the case of PP product ion (Figure 6a), and 1447.0 in the case of PD product ion (Figure 6b). The fragments containing the sulfate-carrying structure appeared at 3 m/z units higher (framed structures, Figure 6). Therefore, B, Y and C, Z fragments on α

antenna all carry the same m/z unit, while those on β antenna and core were observed at 3 m/z unit higher. The $Y_{5\alpha}$ fragment with a theoretical m/z unit of 1606.8 Da was observed at m/z unit values of 1607.3 Da (PP) and 1607.4 Da (PD) in Figure 6a and b, respectively. Elucidation of the sulfate position on the sugar ring requires cross-ring fragmentation on the terminal galactose possessing a sulfate group. Unfortunately, cross-ring fragmentation, especially on the non-reducing end of a glycan structure [40, 41] is usually very difficult to observe due to the high-energy requirement and stereo confinement [39, 42, 43]. By optimizing the CID gas pressure, the cross-ring fragmentation was enhanced to a certain extent. Three cross-ring fragments on the terminal galactose residue (Gal) were observed, including $^{0,4}X_{5\alpha}$ (theoretical m/z unit 1791.9, observed m/z unit 1791.5 (PP and PD)) and an internal fragment $C_5^{2,4}X_{5\alpha}$ (theoretical m/z unit 662.3, observed m/z unit 662.6 (PP and PD)). Detection of these fragments allows the assignment of sulfate at either 3 or 4

Table 3. Structure, m/z values, and diagnostic ions for identified compounds

Compound structure	Calcd m/z [a]	Observed m/z	Diagnostic ions			Determined sulfate position
			Fragment type	Calcd m/z	Observed m/z	
SO3 ▢–■–●–◇–■–▼ (two rows)	2326.0 (PP) 2332.0 (PD)	2326.0 (PP) 2331.9(PD)	Y_5 $Y_{4\alpha/\beta}Y_{5\beta/\alpha}$ $C_{3\alpha}{}^{2,4}X_{5\alpha}$	2067.1(PP) 2070.1(PD) 1563.4 662.3	2067.4(PP) 2070.4(PD) 1563.7 662.5	Terminal GalNAc 3 or 4
SO3 ▢–■–●–◇–■ (two rows)	2152.1 (PP) 2158.1 (PD)	2159.8 (PP) 2157.8 (PD)	$Z_{5\alpha/\beta}Z_{5\beta/\alpha}$-$32$[b] $C_{3\alpha}{}^{2,4}X_{5\alpha}$	1565.8 662.3	1566.0 662.5	Terminal GalNAc 3 or 4
(branched) SO3 ▢–■–●	2069.9 (PP) 2072.8 (PD)	2069.6 (PP) 2072.3 (PD)	$Y_{5\alpha}$ ${}^{3,5}X_{5\alpha}Y_{4\beta}$ $C_{3\alpha}{}^{2,4}X_{5\alpha}$	1811.1 1749.9 662.3	1811.3 1749.6 662.3	Terminal GalNAc 4 or 6
SO3 ▢–■–●–◇–■–▼	2039.9 (PP) 2042.8 (PD)	2039.3 (PP) 2042.3(PD)	$Y_{5\alpha}$ $C_{3\alpha}{}^{2,4}X_{5\alpha}$	1781.1 662.3	1781.3 662.4	Terminal GalNAc 3 or 4
SO3 ▢–■–●–◇–■–■	1906.8 (PP) 1909.8 (PD)	1907.0 (PP) 1910.0 (PD)	$Y_{5\alpha}$ $C_{3\alpha}{}^{2,4}X_{5\alpha}$	1647.7 662.3	1648.0 662.6	Terminal GalNAc 3 or 4
SO3 ▢–■–●–◇–■–■	1865.8 (PP) 1868.8 (PD)	1865.2 (PP) 1868.1 (PD)	$Y_{5\alpha}$ ${}^{0,4}X_{5\alpha}$ $C_{3\alpha}{}^{2,4}X_{5\alpha}$	1606.8 1791.8 662.3	1607.3 1792.1 662.6	Terminal GalNAc 3 or 4
SO3 ▢–■–●–◇–■–▼	1835.9 (PP) 1838.9(PD)	1835.8 (PP) 1838.8 (PD)	$Y_{5\alpha}$	1576.8	1577.1	Terminal GalNAc
SO3 ▢–■–●–◇–■	1661.7 (PP) 1664.7 (PD)	1661.0 (PP) 1664.3 (PD)	$Y_{5\alpha}$	1402.6	1402.8	Terminal GalNAc

[a]All ions including the sulfate groups are sodiated unless otherwise annotated.
[b]The 32 Da loss corresponds to the neutral loss of a CH_3OH group.

position on the sugar ring. However, unambiguous assignment requires a cross-ring fragmentation, involving the breakage of C–C at position 3, which was not observed under the current experimental conditions. Similarly, sulfate group can only be assigned to two possible positions according to the cross-ring fragmentations on all other structures. However, the sulfate-carrying monosaccharides were unambiguously determined for all compounds, being consistent with the published data [31, 32].

The determined structure and diagnostic ions for the major bTSH glycans are summarized in Table 3. Typically, abundant B and Y ions are used to locate the sulfate-carrying monosaccharide, while X ions are used to determine the position on the sugar ring. Interestingly, a peak at 2157.8 Da (PP), which corresponds to a biantennary disulfated structure, was observed only in the doubly-permethylated sample spectra, but not in the only permethylated sample spectra. This confirms again that the ionization is enhanced after the removal of a sulfate group, while the suppressed peaks reappeared after double-permethylation. This result also suggests that double-permethylation can be used to detect otherwise suppressed sulfated glycans.

Conclusions

Double-permethylation enables structural analysis of sulfated glycans in the positive-ion MS mode by substituting sulfate groups with deuteromethyl groups. It allows the determination of sulfate numbers as well as their positions on a glycan. The number of sulfate groups is easily deduced by calculating the mass shift between the permethylated spectra and doubly-permethylated spectra. The position of sulfate groups, on the other hand, can be determined by comparing the CID spectra of PP and PD doubly-permethylated sample. Ionization as well as fragmentation, including cross-ring fragmentation, has also been enhanced through this treatment. As a result, the otherwise suppressed sulfated glycans can be recovered to allow their structural determination. Sample loss due to desulfation reaction is minimal, while all the peaks resulting from the peeling reactions can be excluded by the n × 85 m/z unit mass-shift requirement. As all analyses can be carried out in the positive-ion mode MS, a simultaneous abundance comparison and structural determination of sulfated, sialylated, and neutral

structures become possible. Applications of this method to the comparative studies of the role of sulfated glycans in health and disease are currently being pursued in our laboratory.

Acknowledgments

References

1. Fuster, M. M.; Esko, J. D. The Sweet and Sour of Cancer: Glycans as Novel Therapeutic Targets. *Nat. Rev. Cancer* 2005, *5*(7), 526–542.
2. Varki, A. Biological Roles of Oligosaccharides: All of the Theories Are Correct. *Glycobiology* 1993, *3*(2), 97–130.
3. Ohtsubo, K.; Marth, J. D. Glycosylation in Cellular Mechanisms of Health and Disease. *Cell* 2006, *126*, 855–867.
4. Fukuda, M.; Hiraoka, N.; Akama, T. O.; Fukuda, M. N. Carbohydrate-modifying Sulfotransferases: Structure, Function, and Pathophysiology. *J. Biol. Chem.* 2001, *276*, 47747–47750.
5. Chance, D. L.; Mawhinney, T. P. Disulfated Oligosaccharides. Derived from Tracheobronchial Mucous Glycoproteins of a Patient Suffering from Cystic Fibrosis. *Carbohydr. Res.* 1996, *295*, 157–177.
6. Xiong, L.; Andrews, D.; Regnier, F. Comparative Proteomics of Glycoproteins Based on Lectin Selection and Isotope Coding. *J. Proteome Res.* 2003, *2*(6), 618–625.
7. Hard, K.; Van Zadelhoff, G.; Moonen, P.; Kamerling, J. P.; Vliegenthart, J. F. G. The Asn-linked Carbohydrate Chains of Human Tamm-Horsfall Glycoprotein of One Male. *Eur. J. Biochem.* 1992, *209*, 895–915.
8. Johannes J. M.; van Rooijen, J. P. K.; Vliegenthart, J. F. G. Sulfated Di-, Tri- and Tetraantennary N-glycans in Human Tamm-Horsfall Glycoprotein. *Eur. J. Biochem.* 1998, *256*(2), 471–487.
9. Freeze, H.; Wolgast, D. Structural Analysis of N-Linked Oligosaccharides from Glycoproteins Secreted by *Dictyostelium discoideum*. Identification of mannose 6- sulfate. *J. Biol. Chem.* 1986, *261*(1), 127–134.
10. Green, E. D.; Baenziger, J. U. Asparagine-linked oligosaccharides on lutropin, follitropin, and thyrotropin. I. Structural elucidation of the sulfated and sialylated oligosaccharides on bovine, ovine, and human pituitary glycoprotein hormones. *J. Biol. Chem.* 1988, *263*(1), 25–35.
11. Bowman, K. G.; Cook, B. N.; de Graffenried, C. L.; Bertozzi, C. R. Biosynthesis of L-Selectin Ligands: Sulfation of Sialyl Lewis X-Related Oligosaccharides by a Family of GlcNAc-6-sulfotransferases. *Biochemistry* 2001, *40*(18), 5382–5391.
12. Zaia, J. Mass Spectrometry of Oligosaccharides. *Mass Spectrom. Rev.* 2004, *23*, 161–227.
13. Juhasz, P.; Biemann, K. Mass Spectrometric Molecular-Weight Determination of Highly Acidic Compounds of Biological Significance via Their Complexes with Basic Polypeptides. *Proc. Nat. Acad. Sci. U.S.A.* 1994, *91*(10), 4333–4337.
14. Juhasz, P.; Biemann, K. Utility of Noncovalent Complexes in the Matrix-Assisted Laser Desorption Ionization Mass Spectrometry of Heparin-Derived Oligosaccharides. *Carbohydr. Res.* 1995, *270*(2), 131–147.
15. Harvey, D. J.; Hunter, A. P.; Bateman, R. H.; Brown, J.; Critchley, G. Relationship Between In-Source and Post-Source Fragment Ions in the Matrix-Assisted Laser Desorption (Ionization) Mass Spectra of Carbohydrates Recorded with Reflectron Time-of-Flight Mass Spectrometers. *Int. J. Mass Spectrom.* 1999, *188*(1/2), 131–146.
16. Thomsson, K. A.; Karlsson, N. G.; Hansson, G. C. Liquid Chromatography-Electrospray Mass Spectrometry as a Tool for the Analysis of Sulfated Oligosaccharides from Mucin Glycoproteins. *J. Chromatogr. A* 1999, *854*(1/2), 131–139.
17. Hitchcock, A. M.; Costello, C. E.; Zaia, J. Glycoform Quantification of Chondroitin/Dermatan Sulfate Using a Liquid Chromatography-Tandem Mass Spectrometry Platform. *Biochemistry* 2006, *45*(7), 2350–2361.
18. Liedtke, S.; Geyer, H.; Wuhrer, M.; Geyer, R.; Frank, G.; Gerardy-Schahn, R.; Zahringer, U.; Schachner, M. Characterization of N-glycans from Mouse Brain Neural Cell Adhesion Molecule. *Glycobiology* 2001, *11*(5), 373–384.
19. Geyer, H.; Bahr, U.; Liedtke, S.; Schachner, M.; Geyer, R. Core Structures of Polysialylated Glycans Present in Neural Cell Adhesion Molecule from Newborn Mouse Brain. *Eur. J. Biochem.* 2001, *268*(24), 6587–6599.
20. Xie, Y. M.; Tseng, K.; Lebrilla, C. B.; Hedrick, J. L. Targeted Use of Exoglycosidase Digestion for the Structural Elucidation of Neutral

O-linked Oligosaccharides. *J. Am. Soc. Mass Spectrom.* 2001, *12*(8), 877–884.
21. Tseng, K.; Wang, H.; Lebrilla, C. B.; Bonnell, B.; Hedrick, J. Identification and Structural Elucidation of Lectin-binding Oligosaccharides by Bio-affinity Matrix-assisted Laser Desorption/ionization Fourier Transform Mass Spectrometry. *Anal. Chem.* 2001, *73*(15), 3556–3561.
22. Jiang, H.; Irungu, J.; Desaire, H. Enhanced Detection of Sulfated Glycosylation Sites in Glycoproteins. *J. Am. Soc. Mass Spectrom.* 2005, *16*(3), 340–348.
23. Irungu, J.; Dalpathado, D. S.; Go, E. P.; Jiang, H.; Ha, H.-V.; Bousfield, G. R.; Desaire, H. Method for Characterizing Sulfated Glycoproteins in a Glycosylation Site-Specific Fashion, Using Ion Pairing and Tandem Mass Spectrometry. *Anal. Chem.* 2006, *78*(4), 1181–1190.
24. Imami, K.; Ishihama, Y.; Terabe, S. On-line Selective Enrichment and Ion-pair Reaction for Structural Determination of Sulfated Glycopeptides by Capillary Electrophoresis-mass Spectrometry. *J. Chromatogr. A* 2008, *1194*(2), 237–242.
25. Taguchi, T.; Iwasaki, M.; Muto, Y.; Kitajima, K.; Inoue, S.; Khoo, K. H.; Morris, H. R.; Dell, A.; Inoue, Y. Occurrence and Structural Analysis of Highly Sulfated Multiantennary N-linked Glycan Chains Derived from a Fertilization-Associated Carbohydrate-Rich Glycoprotein in Unfertilized Eggs of *Tribolodon hakonensis*. *Eur. J. Biochem.* 1996, *238*, 357–367.
26. Khoo, K.-H.; Morris, H. R.; McDowell, R. A.; Dell, A.; Maccarana, M.; Lindahl, U. FABMS/Derivatization Strategies for the Analysis of Heparin-derived Oligosaccharides. *Carbohydr. Res.* 1983, *244*(2), 205–223.
27. Cointe, D.; Leroy, Y.; Chirat, F. Determination of The Sialylation Level and of the Ratio α-(2–>3)/α-(2–>6) Sialyl Linkages of N-glycans by Methylation and GC/MS Analysis. *Carbohydr. Res.* 1998, *311*(1/2), 51–59.
28. Kim, Y.-G.; Kim, S.-Y.; Hur, Y.-M.; Joo, H.-S.; Chung, J.; Lee, D.-S.; Royle, L.; Rudd, P. M.; Dwek, R. A.; Harvey, D. J.; Kim, B.-G. The Identification and Characterization of Xenoantigenic Nonhuman Carbohydrate Sequences in Membrane Proteins from Porcine Kidney. *Proteomics* 2006, *6*(4), 1133–1142.
29. Kang, P.; Mechref, Y.; Klouckova, I.; Novotny, M. V. Solid-Phase Permethylation of Glycans for Mass Spectrometric Analysis. *Rapid Commun. Mass Spectrom.* 2005, *19*, 3421–3428.
30. Kang, P.; Mechref, Y.; Novotny, M. V. High-Throughput Solid-Phase Permethylation of Glycans Prior to Mass Spectrometry. *Rapid Commun. Mass Spectrom.* 2008, *22*(5), 721–734.
31. Green, E.; Baenziger, J. Asparagine-Linked Oligosaccharides on Lutropin, Follitropin, and Thyrotropin. I. Structural Elucidation of the Sulfated and Sialylated Oligosaccharides on Bovine, Ovine, and Human Pituitary Glycoprotein Hormones. *J. Biol. Chem.* 1988, *263*(1), 25–35.
32. Baenziger, J. U.; Green, E. D. Pituitary Glycoprotein Hormone Oligosaccharides: Structure, Synthesis, and Function of the Asparagine-Linked Oligosaccharides on Lutropin, Follitropin, and Thyrotropin. *Biochim. Biophys. Acta Rev. Biomembr.* 1988, *947*(2), 287–306.
33. Wheeler, S. F.; Harvey, D. J. Extension of the In-Gel Release Method for Structural Analysis of Neutral and Sialylated N-Linked Glycans to the Analysis of Sulfated Glycans: Application to the Glycans from Bovine Thyroid-Stimulating Hormone. *Anal. Biochem.* 2001, *296*(1), 92–100.
34. Morelle, W.; Donadio, S.; Ronin, C.; Michalski, J.-C. Characterization of N-glycans of Recombinant Human Thyrotropin Using Mass Spectrometry. *Rapid Commun. Mass Spectrom.* 2006, *20*(3), 331–345.
35. Mechref, Y.; Novotny, M. V. Mass Spectrometric Mapping and Sequencing of N-Linked Oligosaccharides Derived from Submicrogram Amounts of Glycoproteins. *Anal. Chem.* 1998, *70*(3), 455–463.
36. Kang, P.; Mechref, Y.; Kyselova, Z.; Goetz, J. A.; Novotny, M. V. Comparative Glycomic Mapping (C-GlycoMAP) through Quantitative Permethylation and Stable-Isotope Labeling. *Anal. Chem.* 2007, *79*, 6064–6073.
37. Ciucanu, I.; Costello, C. E. Elimination of Oxidative Degradation During the Per-O-Methylation of Carbohydrates. *J. Am. Chem. Soc.* 2003, *125*, 16213–16219.
38. Morelle, W.; Faid, V.; Michalski, J.-C. Structural Analysis of Permethylated Oligosaccharides using Electrospray Ionization Quadrupole Time-of-Flight Tandem Mass Spectrometry and deutero-reduction. *Rapid Commun. Mass Spectrom.* 2004, *18*(20), 2451–2464.
39. Domon, B.; Costello, C. E. A Systematic Nomenclature for Carbohydrate Fragmentations in FAB-MS/MS Spectra of Glycoconjugates. *Glycoconj. J.* 1988, *5*(4), 397–409.
40. Cancilla, M. T.; Penn, S. G.; Carroll, J. A.; Lebrilla, C. B. Coordination of Alkali Metals to Oligosaccharides Dictates Fragmentation Behavior in Matrix Assisted Laser Desorption Ionization/Fourier Transform Mass Spectrometry. *J. Am. Chem. Soc.* 1996, *118*(28), 6736–6745.
41. Spengler, B.; Dolce, J. W.; Cotter, R. J. Infrared Laser Desorption Mass Spectrometry of Oligosaccharides: Fragmentation Mechanisms and Isomer Analysis. *Anal. Chem.* 1990, *62*(17), 1731–1737.
42. Mechref, Y.; Baker, A. G.; Novotny, M. V. Matrix-assisted Laser Desorption/ionization Mass Spectrometry of Neutral and Acidic Oligosaccharides with Collision-Induced Dissociation. *Carbohydr. Res.* 1998, *313*(3/4), 145–155.
43. Mechref, Y.; Novotny, M. V.; Krishnan, C. Structural Characterization of Oligosaccharides Using MALDI-TOF/TOF Tandem Mass Spectrometry. *Anal. Chem.* 2003, *75*(18), 4895–4903.